

## Recent studies on vector charmonium(-like) states at BESIII

Yuping Guo<sup>a,\*</sup> on behalf of the BESIII Collaboration

<sup>a</sup>Fudan University,

No.220, Handan Road, Shanghai, China

E-mail: [guoyup@fudan.edu.cn](mailto:guoyup@fudan.edu.cn)

Since the last decade of this century, a number of charmonium-like states, referred to as XYZ states, have been observed in various experiments. They are considered as strong candidates for exotic hadrons, as their properties cannot be accounted for by charmonium states composed of a pair of  $c\bar{c}$ . The vector charmonium-like states have quantum numbers of  $J^{PC} = 1^{--}$ . They can be produced directly from the electron-positron annihilation process. Here, recent studies of vector charmonium-like states by investigating the cross-sections of exclusive processes at BESIII experiment will be presented, including the precise measurements of the cross-sections of  $e^+e^- \rightarrow D\bar{D}$ ,  $e^+e^- \rightarrow D_s^+D_s^-$ ,  $e^+e^- \rightarrow D_s^\pm D_{s1}(2536)^\mp$ ,  $e^+e^- \rightarrow D_s^\pm D_{s2}^*(2573)^\mp$ ,  $e^+e^- \rightarrow \eta h_c$ , and  $e^+e^- \rightarrow \omega \chi_{c1,2}$ . Resonant structures are found in these processes with masses between 4.0 and 4.7 GeV/ $c^2$ .

42nd International Conference on High Energy Physics (ICHEP2024)

18-24 July 2024

Prague, Czech Republic

---

\*Speaker

## 1. Introduction

The Quark Model has proven successful as it clarified all the hadrons known at the time and predicted additional hadrons that have since been discovered. The hadrons observed in the 20th century can be categorized as mesons, composed of one quark and one antiquark, and baryons, which consist of three quarks. The original papers also predicted hadrons with more complex inner structures, such as tetraquark states ( $qq\bar{q}\bar{q}$ ) and pentaquark states ( $qqqq\bar{q}$ ) [1]. Additionally, hadrons composed solely of gluons (glueballs), quarks and excited gluon (hybrids), or groups of hadrons (hadronic molecules) are also allowed. The search for exotic hadrons is a topic of significant interest. However, no candidates were found until the early 21st century.

Since 2003, numerous charmonium-like states have been observed in various experiments. These states exhibit properties that cannot be explained as conventional charmonium states. The vector charmonium-like states ( $J^{PC} = 1^{--}$ ) can be produced at electron-positron colliders either via the direct annihilation process or the initial state radiation (ISR) process. The first vector charmonium-like state,  $Y(4260)$ , is discovered in the ISR process,  $e^+e^- \rightarrow \gamma_{\text{ISR}}\pi^+\pi^-J/\psi$  at BaBar experiment [2]. The mass of  $Y(4260)$  is above the open-charm threshold, but no distinct peak structure is observed in the inclusive hadron cross-section [3], which is abnormal for a charmonium state. Later, the  $Y(4360)$  and  $Y(4660)$  were discovered by the BaBar [4] and Belle experiments [5] respectively, in  $e^+e^- \rightarrow \gamma_{\text{ISR}}\pi^+\pi^-\psi(3686)$  process. Before 2015, four vector charmonium-like states are observed: two decay only into  $\pi^+\pi^-J/\psi$ , while the other two decay into  $\pi^+\pi^-\psi(3686)$ .

The BESIII experiment is situated at the Beijing Electron Positron Collider (BEPCII), which records  $e^+e^-$  collisions in the center-of-mass (c.m.) energy ( $\sqrt{s}$ ) range of 1.84 to 4.95 GeV. The peak luminosity is  $1.1 \times 10^{33} \text{ cm}^{-2}\text{s}^{-1}$ , achieved at  $\sqrt{s} = 3.773 \text{ GeV}$ . Since the end of 2012, BESIII experiment has collected large data samples with  $\sqrt{s}$  above 3.8 GeV to study charmonium(-like) states. These data samples include a scan sample taken at 46 energy points between 3.8 and 4.95 GeV with a total integrated luminosity of  $22 \text{ fb}^{-1}$ , and a scan sample of 104 energy points between 3.8 and 4.6 GeV with a total integrated luminosity of  $826.2 \text{ pb}^{-1}$ . The vector charmonium(-like) states are studied by measuring the cross-sections of exclusive processes. Compared to the ISR approach used in BaBar, CLEO, and Belle experiments, the direct annihilation process used at BESIII offers better precision for studying the vector charmonium(-like) states. This is because the collider operates at and near the c.m. energies corresponding to the resonant peaks and the detection efficiency is generally higher. Over 50 exclusive processes have been precisely measured using (part of) these data samples, significantly enhancing our understanding of the vector charmonium-like states. For instance, the  $Y(4260)$  observed in the ISR process is comprised of  $Y(4230)$  and  $Y(4320)$  [6], and the resonant structure around  $4.23 \text{ GeV}/c^2$  is also observed in other hidden charm and open charm processes, such as  $e^+e^- \rightarrow \pi^+\pi^-h_c$  [7],  $e^+e^- \rightarrow K^+K^-J/\psi$  [8], and  $e^+e^- \rightarrow \pi^\pm(D^{(*)}\bar{D}^*)^\mp$  [9, 10]. In this paper, five selected studies of vector charmonium-like states will be presented, charge conjugated modes are implied throughout this paper.

## 2. Precise measurements of the cross-section of $e^+e^- \rightarrow D\bar{D}$ and $e^+e^- \rightarrow D_s^+D_s^-$

A striking feature of the charmonium-like states is their small coupling to open charm final states. It is crucial to investigate the coupling of charmonium-like states to open charm channels,

which requires precise measurement of the cross-sections.

The study of the cross-section of  $e^+e^- \rightarrow D\bar{D}$  is conducted by using data samples collected at 150 c.m. energies at  $\sqrt{s}$  between 3.80 and 4.95 GeV, corresponding to an integrated luminosity of  $20 \text{ fb}^{-1}$  [11]. Both  $D^0\bar{D}^0$  and  $D^+D^-$  processes are studied. A single tag technique is employed to increase the statistics, only one  $D^0$  ( $D^+$ ) meson is reconstructed using the  $K^-\pi^+\pi^-\pi^+$  ( $K^-\pi^+\pi^+$ ) decay mode, while the corresponding antiparticle is extracted from the recoil side. The signal yields are extracted by performing fit to the modified  $M_D^{\text{recoil}}$  spectrum,  $M_D^{\text{recoil}} + M_D - m_D$ , which eliminated the mass resolution of the tagged  $D$  meson. The Born cross-sections of  $e^+e^- \rightarrow D\bar{D}$  are shown in Fig. 1. The precision achieved in this study is unprecedented, with total systematic uncertainties of 7.0% for the  $D^0\bar{D}^0$  mode and 6.5% for the  $D^+D^-$  mode. Clear peaks can be identified in the cross-section line shape around the mass range of  $G(3900)$ ,  $\psi(4040)$ ,  $\psi(4160)$ ,  $\psi(4260)$ , and  $\psi(4415)$ . Determination of the coupling of these vector states to  $D\bar{D}$  mode needs a coupled-channel analysis.

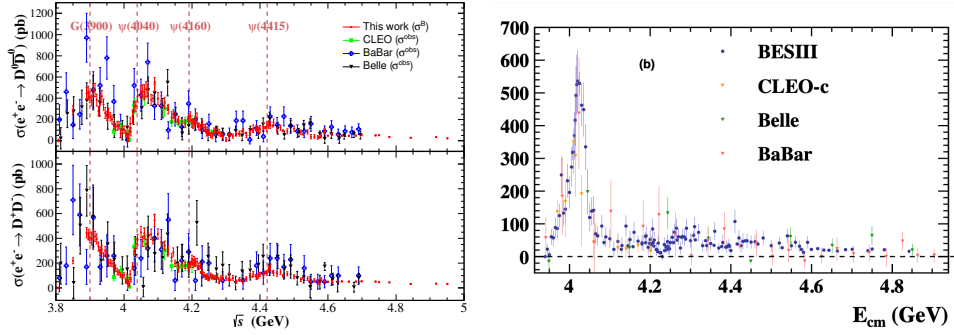


**Figure 1:** (Left) The Born cross section of  $e^+e^- \rightarrow D\bar{D}$  from BESIII experiment, compared with the observed cross-section from previous measurements. (Right) The Born cross section of  $e^+e^- \rightarrow D_s^+ D_s^-$  from BESIII experiment, compared with the Born cross-section from previous measurements.

The cross-section of  $e^+e^- \rightarrow D_s^+ D_s^-$  is measured with a similar single tag technique using data samples collected at 138 c.m. energies at  $\sqrt{s}$  between 3.94 and 4.95 GeV, corresponding to an integrated luminosity of  $22.9 \text{ fb}^{-1}$  [12]. The  $D_s^-$  meson is reconstructed using the  $\phi(\rightarrow K^+ K^-)\pi^-$  and  $K^*(892)^0(\rightarrow K^+ \pi^-)K^-$  modes. The signal yields are extracted by performing fit to the  $K^+ K^- \pi$  invariant mass spectrum after requiring that the recoil mass of the tagged  $K^+ K^- \pi$  system is within the  $D_s$  mass region. The Born cross section of  $e^+e^- \rightarrow D_s^+ D_s^-$  is shown in Fig. 1. The total systematic uncertainty is 5.5%. Two important features are evident from the cross-section line shape: first, there is a narrow dip around  $\sqrt{s} = 4.23 \text{ GeV}$ , which is near the  $D_s^{*+} D_s^{*-}$  threshold and the peak of the  $Y(4230)$ ; second, the cross-section line shape exhibits structural similarities to the previously reported  $e^+e^- \rightarrow D_s^{*+} D_s^{*-}$  process [13] above 4.4 GeV. A fit to the Born cross-section ratio  $\sigma[e^+e^- \rightarrow D_s^+ D_s^-]/\sigma[e^+e^- \rightarrow D_s^{*+} D_s^{*-}]$  with a constant value leads to a  $\chi^2/\text{ndf} = 1.09$ , while a possible structure around 4.79 GeV is suggested in the  $e^+e^- \rightarrow D_s^{*+} D_s^{*-}$  process.

### 3. Production properties of $D_{s1}(2536)$ and $D_{s2}^*(2573)$

Using data samples collected at 15 c.m. energies ranging from  $\sqrt{s} = 4.530$  to 4.946 GeV, the decay and production properties of  $D_{s1}(2536)$  and  $D_{s2}^*(2573)$  are studied [14]. The produc-

tion properties are analyzed from the cross-section line shapes of  $e^+e^- \rightarrow D_s^- D_{s1}(2536)^+$  and  $D_s^- D_{s2}^*(2573)^+$ . A partial reconstruction method is employed to enhance statistics, wherein a  $D_s^-$  meson is reconstructed through the decays  $D_s^- \rightarrow \phi(\rightarrow K^+ K^-) \pi^-$ ,  $D_s^- \rightarrow K^*(892)^0(\rightarrow K^+ \pi^-) K^-$ , and  $D_s^- \rightarrow K_S^0(\rightarrow \pi^+ \pi^-) K^-$  and a  $K^+$  is selected from the charged tracks that do not form the  $D_s^-$ . The recoil mass of the tagged particles is required to be around the  $D^{*0}$  or  $D^0$  nominal mass for the two decay modes. The yields for  $D_{s1}(2536)$  and  $D_{s2}^*(2573)$  signal events are extracted by performing fit to the recoil mass spectrum of tagged  $D_s$  meson.

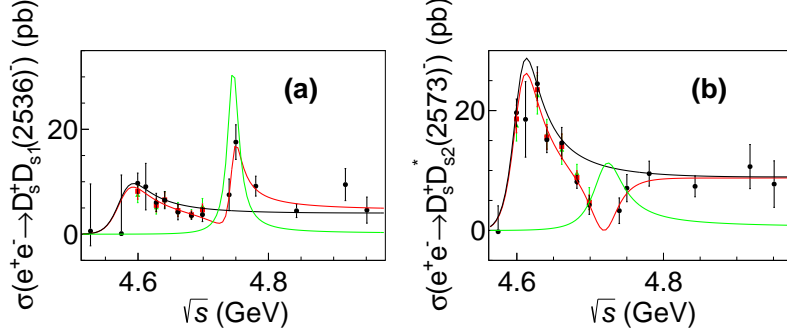


**Figure 2:** (Left) The cross-section of  $e^+e^- \rightarrow D_s^- D_{s1}(2536)^+$  with  $D_{s1}(2536) \rightarrow D^{*0} K$ . (Right) The cross-section of  $e^+e^- \rightarrow D_s^- D_{s2}^*(2573)^+$  with  $D_{s2}^*(2573) \rightarrow D^0 K$ .

The Born cross-sections of the two processes are displayed in Fig. 2, clear peak structures can be found in the cross-section line shapes. The resonant structures are studied by performing least- $\chi^2$  fits to the measured cross-sections with a coherent sum of two constant-width Breit-Wigner (BW) functions. Both processes reveal a resonant structure with statistical significance above  $5\sigma$  in the vicinity of 4.6 GeV and a width of 50 MeV. The second structure in  $e^+e^- \rightarrow D_s D_{s1}(2536)$  process appears around 4.75 GeV with a width of 25 MeV, while for  $e^+e^- \rightarrow D_s D_{s2}^*(2573)$ , it is around 4.72 GeV with a width of 50 MeV. The statistical significances of the second structure are  $4.3\sigma$  and  $2.7\sigma$ , respectively. The resonant structure near 4.6 GeV in  $e^+e^- \rightarrow D_s D_{s2}^*(2573)$  is observed for the first time, and aligns with the  $Y(4620)$  evidence reported in the same final state by the Belle experiment using the ISR approach. The first structure observed in  $e^+e^- \rightarrow D_s D_{s1}(2536)$  process likely corresponds to the  $Y(4626)$  observed by the Belle experiment. The second structure around 4.75 GeV may relate to the  $Y(4710)$  or  $Y(4790)$  observed by BESII in  $e^+e^- \rightarrow K^+ K^- J/\psi$  [8] or  $e^+e^- \rightarrow D_s^{*+} D_s^{*-}$  [13] processes.

#### 4. Measurement of the cross-section of $e^+e^- \rightarrow \eta h_c$ and $e^+e^- \rightarrow \omega \chi_{c1,2}$

The BESIII experiment previously observed the  $e^+e^- \rightarrow \eta h_c$  process using data sample at  $\sqrt{s} = 4.23$  GeV, as well as the  $e^+e^- \rightarrow \omega \chi_{c1}$  and  $\omega \chi_{c2}$  processes at  $\sqrt{s} = 4.60$  GeV and 4.42 GeV, respectively. The cross-section line shapes for these processes show interesting structures; however, the limited data samples hindered detailed studies of the resonant structures. These three processes have been updated using new scan samples between 4.13 and 4.95 GeV accordingly.

Data samples collected at  $\sqrt{s}$  between 4.13 and 4.60 GeV, with an integrated luminosity of  $15 \text{ fb}^{-1}$ , are used for the  $e^+e^- \rightarrow \eta h_c$  process. The  $h_c$  state is reconstructed from its radiative decay

$h_c \rightarrow \gamma\eta_c$  and  $\eta$  from  $\gamma\gamma$ . The  $\eta_c$  is reconstructed with sixteen hadronic final states with a total branching fraction of about 40%. All final state particles are required to be reconstructed to improve signal-to-background ratio. The signal yields are extracted by fitting to the invariant mass spectrum of  $\gamma\eta_c$ . The Born cross-section measured for each sample is shown in Fig. 3. A peak structure is observed near 4.2 GeV. The mass and width of the resonant structure are determined by performing a maximum likelihood fit to the cross-section using the model  $|\text{BW}_1(s) + \text{BW}_2(s)e^{i\phi}|^2 + |\text{BW}_3(s)|^2$ . The parameters of  $\text{BW}_2$  are fixed to those of  $Y(4360)$  due to the large uncertainties of the cross-sections in that region, while the parameters of the other two BW functions are free. The mass and width of the first resonance are determined to be  $M = (4188.8 \pm 4.7 \pm 8.0) \text{ MeV}/c^2$  and  $\Gamma = (49 \pm 16 \pm 19) \text{ MeV}$ , and coupling strength is determined to be  $\Gamma_{ee}\mathcal{B} = (0.80 \pm 0.19 \pm 0.45) \text{ eV}$ . The statistical significance of the first resonance is  $8\sigma$ . The parameters of this resonance are consistent with those of  $\psi(4160)$  and a  $1^{--}$  hybrid charmonium state predicted by the BOEFT model, which has a mass of  $(4.15 \pm 0.15) \text{ GeV}$ . Different parameterizations of the cross-section line shape are tested to check the stability of the first resonance, including changing the parameters of  $\text{BW}_2$  to  $Y(4320)$ ,  $Y(4380)$ , and  $Y(4390)$ , removing the second resonance from the model, and changing the fit model to a sum of a BW function and phase space, or to a coherent sum of three BW functions. In all alternative models, the significance of the first resonance remains above  $7.0\sigma$ .

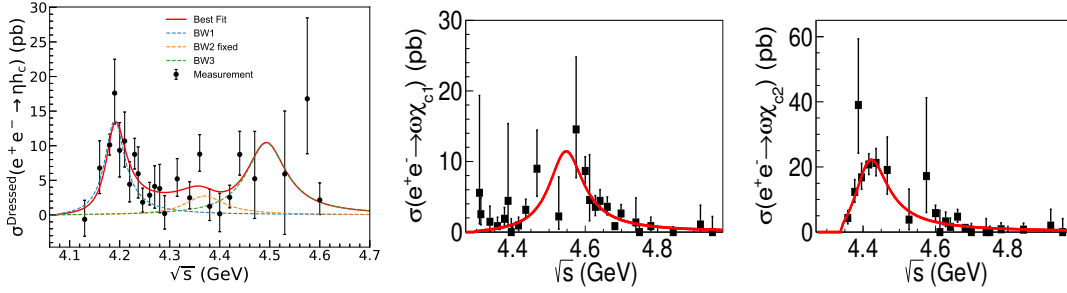


**Figure 3:** The cross-sections of  $e^+e^- \rightarrow \eta h_c$  (left),  $e^+e^- \rightarrow \omega\chi_{c1}$  (middle), and  $e^+e^- \rightarrow \omega\chi_{c2}$  (right) and the best fit results.

The  $e^+e^- \rightarrow \omega\chi_{c1,2}$  processes are updated with scan data sample taken at  $\sqrt{s}$  between 4.30 and 4.95 GeV with an integrated luminosity of  $11 \text{ fb}^{-1}$ . The  $\chi_{c1,2}$  are reconstructed via  $\chi_{c1,2} \rightarrow \gamma J/\psi$  with  $J/\psi \rightarrow e^+e^-$  and  $\mu^+\mu^-$ , and the  $\omega$  is reconstructed from its decay  $\omega \rightarrow \pi^+\pi^-\pi^0 (\rightarrow \gamma\gamma)$ . The signal yields are determined by fitting the invariant mass spectrum of  $\gamma J/\psi$ . The Born cross-sections from the two processes are illustrated in Fig. 3. The cross-section of  $e^+e^- \rightarrow \omega\chi_{c1}$  shows enhancement around 4.5 GeV, while cross-section of  $\omega\chi_{c2}$  process peaks around 4.4 GeV. Assuming one resonant structure for each process, the cross-section line shapes are fitted using maximum likelihood method. The resonant structure is described by a constant-width BW function. The parameters of the resonance for  $\omega\chi_{c1}$  process are  $M = (4544.2 \pm 18.7 \pm 1.7) \text{ MeV}/c^2$ ,  $\Gamma = (116.1 \pm 33.5 \pm 1.7) \text{ MeV}$ , and  $\Gamma_{ee}\mathcal{B} = (1.86 \pm 0.32 \pm 0.13) \text{ eV}$ , those for  $\omega\chi_{c2}$  process are  $M = (4413.6 \pm 9.0 \pm 0.8) \text{ MeV}/c^2$ ,  $\Gamma = (110.5 \pm 15.0 \pm 2.9) \text{ MeV}$ , and  $\Gamma_{ee}\mathcal{B} = (3.17 \pm 0.39 \pm 0.24) \text{ eV}$ . The statistical significances of the resonance over the phase space term are  $5.9\sigma$  and  $10.7\sigma$  for  $\omega\chi_{c1}$  and  $\omega\chi_{c2}$  processes, respectively. The mass of the resonance observed in  $\omega\chi_{c1}$  process is significantly higher than the structures observed around 4.5 GeV in  $e^+e^- \rightarrow K^+K^-J/\psi$  [8] and

$e^+e^- \rightarrow \pi^\pm(D^*\bar{D}^*)^\mp$  [10] processes, further measurements with higher precision are required to identify whether they are the same state. The resonance observed in  $\omega\chi_{c2}$  process is consistent with  $\psi(4415)$ , suggesting the existence of  $\psi(4415) \rightarrow \omega\chi_{c2}$ .

## 5. Summary

Benefiting from the fine scan samples collected at more than 150 c.m. energies ranging from 3.8 to 4.95 GeV at BESIII experiment, the properties of the vector charmonium(-like) states have been investigated in dense using exclusive processes. Five recent studies of the cross-section line shapes are presented in this paper, showcasing the most precise measurements of two-body production of open charm process, along with the observation of resonant structures in the  $\eta h_c$  and  $\omega\chi_{c1,2}$  processes. With the BEPCII upgrade this summer, the luminosity at  $\sqrt{s} = 4.7$  GeV is expected to increase by a factor of 3, and the maximum c.m. energy will reach 5.6 GeV starting in 2028. This upgrade will ultimately enhance statistics for studying charmonium and charmonium-like states in this region, thus deepening our understanding of the nature of the charmonium-like states.

## References

- [1] Gell-Mann M. (1964), [Phys. Lett. \*\*8\*\*, 214 \(1964\)](#). Zweig G. (1964), [CERN-TH.401,\(1964\)](#).
- [2] Aubert B. *et al.* (BABAR Collaboration) (2005), [Phys. Rev. Lett. \*\*95\*\*, 142001 \(2005\)](#).
- [3] Ablikim M. *et al.* (BES Collaboration) (2008), [Phys. Lett. B \*\*660\*\*, 315 \(2008\)](#).
- [4] Aubert B. *et al.* (BABAR Collaboration) (2007), [Phys. Rev. Lett. \*\*98\*\*, 212001 \(2007\)](#).
- [5] Wang X. L. *et al.* (Belle Collaboration) (2007), [Phys. Rev. Lett. \*\*99\*\*, 142002 \(2007\)](#).
- [6] Ablikim M. *et al.* (BESIII Collaboration) (2017), [Phys. Rev. Lett. \*\*118\*\*, 092001 \(2017\)](#).
- [7] Ablikim M. *et al.* (BESIII Collaboration) (2017), [Phys. Rev. Lett. \*\*118\*\*, 092002 \(2017\)](#).
- [8] Ablikim M. *et al.* (BESIII Collaboration) (2022), [Chin. Phys. C \*\*46\*\*, 111002 \(2022\)](#). Ablikim M. *et al.* (BESIII Collaboration) (2023), [Phys. Rev. Lett. \*\*131\*\*, 211902 \(2023\)](#).
- [9] Ablikim M. *et al.* (BESIII Collaboration) (2019), [Phys. Rev. Lett. \*\*122\*\*, 102002 \(2019\)](#).
- [10] Ablikim M. *et al.* (BESIII Collaboration) (2023), [Phys. Rev. Lett. \*\*130\*\*, 121901 \(2023\)](#).
- [11] Ablikim M. *et al.* (BESIII Collaboration) (2024), [Phys. Rev. Lett. \*\*133\*\*, 081901 \(2024\)](#).
- [12] Ablikim M. *et al.* (BESIII Collaboration) (2024), [arXiv:2403.14998 \(2024\)](#).
- [13] Ablikim M. *et al.* (BESIII Collaboration) (2023), [Phys. Rev. Lett. \*\*131\*\*, 151903 \(2023\)](#).
- [14] Ablikim M. *et al.* (BESIII Collaboration) (2024), [arXiv:2407.07651 \(2024\)](#).
- [15] Ablikim M. *et al.* (BESIII Collaboration) (2024), [arXiv:2404.06718 \(2024\)](#).
- [16] Ablikim M. *et al.* (BESIII Collaboration) (2024), [Phys. Rev. Lett. \*\*132\*\*, 161901 \(2024\)](#).